Non-intrusive implementation of the Generalized Finite Element Method with Global-Local Enrichment for multi-domain analysis

Túlio Roberto Eládio Marques[1], Ana Clara Pedras Bueno[1], Ramon Pereira da Silva[1], Felício Bruzzi Barros[1]

[1]*Dept. of Structural Engineering, Federal University of Minas Gerais*
Av. Antônio Carlos, 6627 – Pampulha, 31270-901, Minas Gerais, Brazil
tulioeladio10@ufmg.br, anaclarabueno@ufmg.br, ramon@ufmg.br, felicio@ufmg.br

Abstract. This work presents a non-intrusive implementation of the Generalized Finite Element Method with Global-Local enrichment (IGL-GFEM^{gl}) for multi-domain analysis. In IGL-GFEM^{gl}, the global problem is initially discretized using a coarse mesh, without considering localized phenomena. In this work, the solution of this domain is obtained using the commercial software *Abaqus*. Following, mesoscales, as many as necessary, are defined. The global-local enrichment of the GFEM^{gl} determines the association of each mesoscale with its respective local problem, if it exists. The coupling between mesoscales and the global problem is established through the transfer of displacements and generalized forces, defining the non-intrusive strategy denominated Iterative Global-Local (IGL). Numerical simulations using GFEM and GFEM^{gl} are executed in the computational system *INSANE* (INteractive Structural ANalysis Enviroment - www.insane.dees.ufmg.br). The combination of solvers, indicated in the solution methodology, focuses on endorsing the application of academic algorithms as instruments with the capacity to solve complex models utilizing commercial software. A numerical example is presented to demonstrate the simulation's performance and to investigate the influence of the main parameters related to the proposed strategy. This work is part of a master's research in development that proposes the expansion of the implementation of the non-intrusive strategy in *INSANE*.

Keywords: Generalized Finite Element Method, Coupling strategies, Fracture Mechanics, Multi-domain analysis

1 Introduction

A wide range of solid mechanic problems involves complex physical phenomena, such as cracks and high stress gradients. Typically, these phenomena manifest in well-defined regions, motivating refined investigation only in these domain areas. Several computational methods have been developed to solve multiscale or domain decomposition problems, such as the Iterative Global-Local - IGL [1].

An important characteristic of the IGL approach is the non-intrusive coupling, which allows commercial software to use algorithms developed in research environments. This method provides the industry with advanced formulations, such as the Generalized Finite Element Method - GFEM [2] and its Global-Local approach - GFEM^{gl} [3], in combination with a robust software widely used by project engineers.

In GFEM, FEM conventional shape functions are multiplied by enrichment functions, improving the model representation. Added to this improvement, in GFEM^{gl}, the problem solution is divided into three steps and two scales, beginning with a coarse discretization of the entire domain. Subsequently, a local problem defined in a region with singularities in the displacement gradients (such as cracks) is solved, starting from the imposition of the results obtained as boundary conditions. This strategy is concluded with a reanalysis of the initial problem enriched with the solution obtained in the local problem. In GFEM^{gl}, the remeshing of the global domain is dismissed, due to the introduction of the local numerical solution in the initial problem through enrichment functions.

Li et al. [4] present IGL-GFEM^{gl}, combining the non-intrusive implementation (IGL) with GFEM^{gl} for the analysis of multiscale problems. This method differs from its predecessors, which the coupling strategy relied on substructuring algorithms, static condensation of the global stiffness matrix and *Schwarz* algorithms [5]. In Li et al. [4]'s approach the problem is divided into three scales. The entire problem domain is considered to simulate its global behavior by the *Abaqus* software. On a local scale, the phenomenon of interest is analyzed by a research software. An intermediate scale, called mesoscale, integrates the global and local scales of analysis. The mesoscale interacts with the local scale through the GFEM^{gl} approach, while the interaction with the global scale is defined by the IGL strategy. In this work, the coupling (implemented in [6], [7]), considering *Abaqus* and the

INSANE computational platform, is adapted and evaluated for analyzing multiple domains with the presence of local phenomena. This represents the first step toward automating and parallelizing this simulation process using IGL-GFEM^{gl} for multiple analysis domains.

After this introduction, the formulation aspects of IGL-FEM and its variations are presented in Section 2. Then, in Section 3, the numerical experiments are exposed. Finally, the main conclusions of this article are summarized in Section 4.

2 Formulation Aspects

This section presents the main aspects of the IGL-FEM formulation and the simulation of singularities via GFEM.

2.1 Iterative Global-Local Finite Element Method (IGL-FEM)

The IGL-FEM solution procedure is shown in Figure 1(a) and described in detail below:

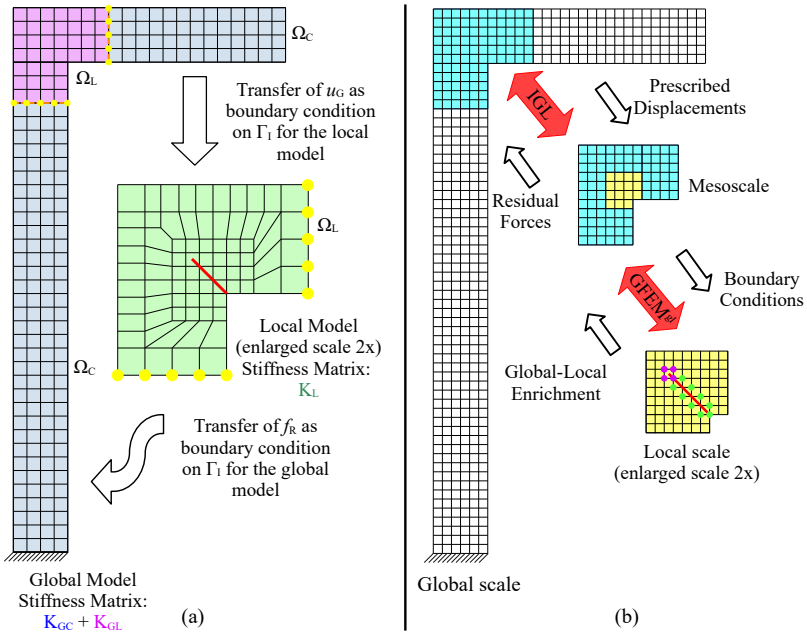

Figure 1. Schematic representation of the solution process via (a)IGL-FEM and (b)IGL-GFEM^{gl}. The components of the interface region, Γ_I, between the local and complementary domains are highlighted in yellow.

1. Global analysis: solve the global model obtaining the initial solution $\mathbf{u_G^0}$;

$$(\mathbf{K_{GC}} + \mathbf{K_{GL}}) \cdot \mathbf{u_G^0} = \mathbf{f_G} \tag{1}$$

2. Local analysis: define and solve the local models to obtain the solution $\mathbf{u_L^k}$. In this step, the initial solution, $\mathbf{u_G^0}$, is used as a boundary condition along the Γ_I interface of each local model;
3. Calculation of residues: from the solutions $\mathbf{u_G^i}$ and $\mathbf{u_L^i}$ associated with the iteration i, calculate the reactions and internal nodal forces on the perimeter Γ_I for the global problem (Ω_C) and the local problem (Ω_L), respectively. The residue vector, obtained from the difference between these forces, is used to update the force vector of the global model;

$$\begin{aligned} f_R = -(\mathbf{f_L^{\Gamma_I}} + \mathbf{f_C^{\Gamma_I}}) = -[(\mathbf{K_L} \cdot \mathbf{u_L^i} - \mathbf{f_L}) \,|_{\mathbf{\Gamma_I}} + \\ (\mathbf{K_{GC}} \cdot \mathbf{u_{GC}}^{\mathbf{i}} - \mathbf{f_{GC}}) \,|_{\mathbf{\Gamma_I}}] \end{aligned} \tag{2}$$

where f_L and f_{GC} are the force vectors associated with contour Γ_I, referring to the local and global models, respectively.

4. Check if the convergence criterion was reached. Otherwise, the iterative process continues by updating the global model (through the addition of the residue $\mathbf{f_R}$ to the global model's force vector via Equation (1));
5. i global-local iteration: return to step 1 to obtain a new solution $\mathbf{u_G^i}$ for the global problem and repeat the other steps described, with the goal to achieve convergence (compatibility of displacements and balance of forces in Γ_I) and the final solution.

The final solution is the combination of the global and local solutions as follows: $\mathbf{u_{GC}}$ (displacements from the global solution, $\mathbf{u_G}$, corresponding to the nodes of the complementary domain) valid in the domain Ω_C and $\mathbf{u_L}$ (from the solution of the local problem) valid in the domain Ω_L. At the interface between the domains, the solution is coincident, as indicated in step 5 of the solution procedure.

2.2 IGL-GFEM^{gl}

In the IGL-GFEM^{gl} strategy proposed by Li et al. [4], the problem is divided into three scales:

- **Global Scale**: represents the entire domain without localized phenomena of interest, discretized with a coarse mesh.
- **Mesoscale**: corresponds to specific subregions of the global scale, with the function of enabling non-intrusive coupling between global and local scales, acting as transition models.
- **Local Scale**: corresponds to the regions where local phenomena and other features of the problem are represented. It is discretized with a refined mesh.

As shown in Figure 1(b), the global scale is coupled through the IGL algorithm to the mesoscale, which is enriched with the local scale solution via GFEM^{gl}. This approach is denominated as a monolithic solution procedure [8]. Li et al. [8] proposed a variant of the IGL-GFEM^{gl} called staggered algorithm. The distinction in this strategy lies in performing IGL [1] cycles between the global model and the mesoscale before the GFEM^{gl} solution, which occurs only after reaching a convergence criterion.

According to Duarte and Kim [3], the hierarchical property of global-local enrichment guarantees that the FEM shape functions remain unchanged after the enrichment, enabling non-intrusive coupling between the global and local problem (defined as mesoscale). The main limitation of this method is associated with non-convergence behavior, since the IGL characteristics are inherited [6]. The creation of a third domain (the local) and the use of global-local enrichment of GFEM^{gl} are not essential to the solution process, arranging to directly couple the IGL algorithm and the GFEM conventional formulation.

2.3 Simulation of singularities through GFEM

The adoption of the GFEM enrichment in problems involving singularities in the stress field is possible through asymptotic functions (suitable for addressing variables whose gradients tend to infinity), to improve the solution in the neighborhood of singular points [9]. The Equations (3) to (6) express these functions:

$$u_x^{(1)} = \frac{1}{2G} r^{\lambda^{(1)}} [(\overline{\kappa} - Q^{(1)}(\lambda^{(1)} + 1)) \cos \lambda^{(1)}\theta \quad - \lambda^{(1)} \cos(\lambda^{(1)} - 2)\theta] \tag{3}$$

$$u_y^{(1)} = \frac{1}{2G} r^{\lambda^{(1)}} [(\overline{\kappa} + Q^{(1)}(\lambda^{(1)} + 1)) \sin \lambda^{(1)}\theta \quad + \lambda^{(1)} \sin(\lambda^{(1)} - 2)\theta] \tag{4}$$

$$u_x^{(2)} = \frac{1}{2G} r^{\lambda^{(2)}} [(\overline{\kappa} - Q^{(2)}(\lambda^{(2)} + 1)) \sin \lambda^{(2)}\theta \quad - \lambda^{(2)} \sin(\lambda^{(2)} - 2)\theta] \tag{5}$$

$$u_y^{(2)} = -\frac{1}{2G} r^{\lambda^{(2)}} [(\overline{\kappa} + Q^{(2)}(\lambda^{(2)} + 1)) \cos \lambda^{(2)}\theta \quad + \lambda^{(2)} \cos(\lambda^{(2)} - 2)\theta] \tag{6}$$

where:

- G is the modulus of rigidity;
- $\overline{\kappa} = (3 - 4\nu)$ for the Plane Strain and $\frac{(3-\nu)}{1+\nu}$ for the Plane Stress, with ν corresponding to Poisson's ratio;
- $\lambda^{(i)}$, $Q^{(i)}$ are constants that depends on the opening angle of the contour at the singular point;
- r and θ are variables in polar coordinates with origin at the singular point.

In the kinematic simulation of cracks in Two-Dimensional Linear Elastic Fracture Mechanics problems, the enrichment can include singularity functions and the Heaviside function - Equation (7) [10] (implemented in *INSANE* by Fonseca [11]).

$$H(\xi) = 1 \,\forall\, \xi > 0; \qquad H(\xi) = 0 \,\forall\, \xi < 0 \tag{7}$$

where ξ represents the position in relation to the discontinuity starting at $\xi = 0$.

3 Numerical Experiments

3.1 Axially tensioned bar

Figure 2 illustrates the first problem studied in this work: an axially tensioned bar ($P = 150$) with the following properties: cross-sectional area $A = 0.5$, Poisson's ratio $\nu = 0.3$, and Young's modulus $E = 200$. Consistent units are adopted. Through the application of the weights α and β to the modulus of elasticity, eight models are simulated, each differing by stiffness loss in certain regions of the domain. Local domains are strategically defined in these regions.

Models 1, 2 and 3 have only one local model, while the others models have two. This example was solved using the IGL solution strategy (Section 2.1) to evaluate the impact of multiple local domains on the solution process convergence. The values for α and β used for each analyzed model and the results obtained are presented in Table 1.

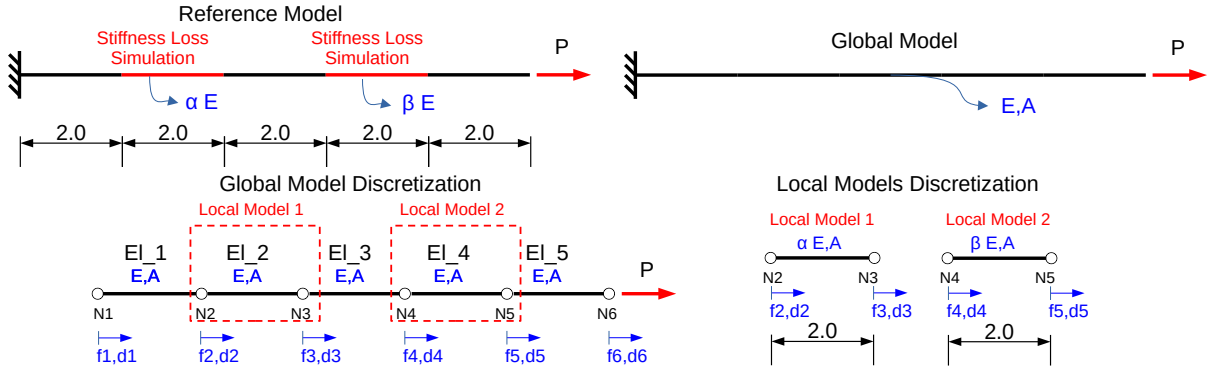

Figure 2. Analysis model and discretization used for the axially tensioned bar

The displacement error at the free end of the cantilever beam (Δ_6) was measured and compared with the reference models. In all cases, the results were satisfactory. Accordingly to the data, the IGL strategy convergence strongly depends on the stiffness variation between the analysis domains (global and local). Comparing the results of models 1, 2 and 3 with models 4, 5 and 6, respectively, it is notable that adding a new local model with the same stiffness penalization does not affect the number of iterations required for convergence.

From models 7 and 8, it is noticeable that the number of IGL iterations performed is defined by convergence conditions of the local domain which implies in a greater stiffness penalization. In these analyses, the domain whose weight is smaller converges faster, and its solution is not affected by the iterations required for the remaining domain convergence. Therefore, the mutual influence between the different local models does not need to be a concern. Any potential interferences can be addressed later in the global problem.

Table 1. α and β parameters and results for each model of problem 1. Models 1, 2 and 3 present only one local problem (related to α).

Model	1	2	3	4	5	6	7	8
α	0.25	0.50	0.75	0.25	0.50	0.75	0.50	0.50
β	-	-	-	0.25	0.50	0.75	0.75	0.25
IGL Iterations	44	17	8	44	17	8	16	42
Error - Δ_6(%)	1.06E-04	1.27E-04	9.54E-05	3.09E-04	2.18E-04	1.80E-04	2.41E-04	1.89E-04

The error evolution can be evaluated by the ratio modulus between the norms of the residue and the reference vectors. The reference vector is calculated using the end forces of the local domain from the first iteration. The

results are presented in Figure 3.

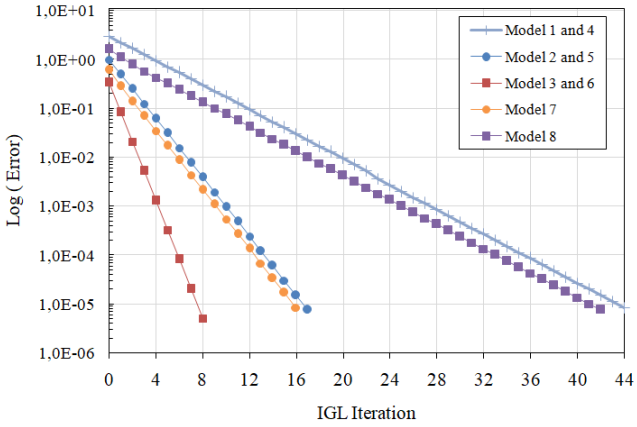

Figure 3. Error associated with iterations

3.2 Plane Frame Model

The second numerical example, solved using IGL-GFEM^{gl}, is presented in Figure 4 and corresponds to a plane frame with a 2.1×10^4 nodal load applied in the element symmetry axis. The elastic material properties are Young's modulus $E = 2.0 \times 10^7$ and Poisson's ratio $\nu = 0.3$. Consistent units are adopted.

The global scale and each mesoscale mesh consists of 1008 and 96 four-node quadrilateral elements (dimensions of 5.0 x 5.0), respectively. Two mesoscales are evaluated. Mesoscale 1 includes a crack defined by the parameters $a = 7.9057$ and $\beta = 2.8198$ represented kinematically in the local model, automatically generated from the strategy implemented in *INSANE* by Fonseca [11]. Mesoscale 2 features eight nodes enriched with singularity functions - eqs. (3 -6) - to represent the displacement and stress fields in the neighborhood of the singular point (corner of the frame).

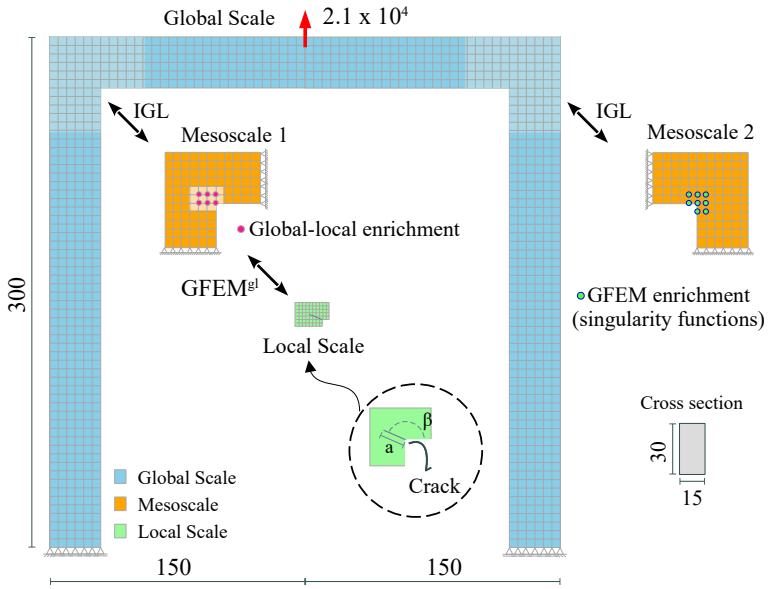

Figure 4. Analysis model and discretization used for the plane frame

The main results are summarized in Table 2: Stresses Intensity Factors - K_I and K_{II} - and Strain Energy - U. The error evolution at each IGL iteration is shown in Figure 5. These data are compared with an equivalent numerical model (global and local problems with equivalent discretizations) solved in *INSANE* environment by GFEM^{gl}.

Two approaches were evaluated: the monolithic and the staggered algorithm (Section 2.2), with convergent results. Notably, for models with five global-local cycles per iteration, the staggered algorithm reduced computational time by 9.94%, due to a lower total number of cycles: 20 versus 25 in the monolithic approach. However, as suggested by Li et al. [4], just one cycle is sufficient to address the effects of low-accurate boundary conditions applied to the local model, emphasizing the monolithic procedure use.

Table 2. Results and respective errors for each model of problem 2

Models	K_I	Error (%)	K_{II}	Error (%)	U	Error (%)	Time(s)	IGL It.	Stag. It.
Reference	726.88	-	5.21	-	73.08	-	248	-	-
Monolithic (1GL)	707.71	2.64	4.99	4.27	72.85	0.31	361	6	-
Monolithic (5GL)	707.73	2.63	4.99	4.22	72.86	0.31	1046	6	-
Staggered (1GL)	707.67	2.64	4.98	4.37	72.85	0.31	587	11	4
Staggered (5GL)	707.67	2.64	4.98	4.38	72.85	0.31	942	11	4

To extend the conclusions of Section 3.1, regarding the unidimensional bar, to plane models, it was studied a frame that contains only mesoscale 1 (intermediate domain of greater complexity of this problem), with 9 IGL iterations and 3 staggered cycles and 6 IGL iterations in the monolithic approach. Comparing these results with those in Table 2, the conclusions observed in Section 3.1 are verified, i.e., the number of iterations required for convergence when added more local domains (here called mesoscales), with less difference in stiffness, is maintained.

Before the first global-local cycle and consideration of the crack (IGL iteration 2 = staggered 1 - Figure 5), an increase of 2 IGL iterations in the staggered approach was observed. This does not represent mutual interference between mesoscales, these additional iterations are required due to the imbalance caused by the enrichment of the GFEM in mesoscale 2, included from the initial stage.

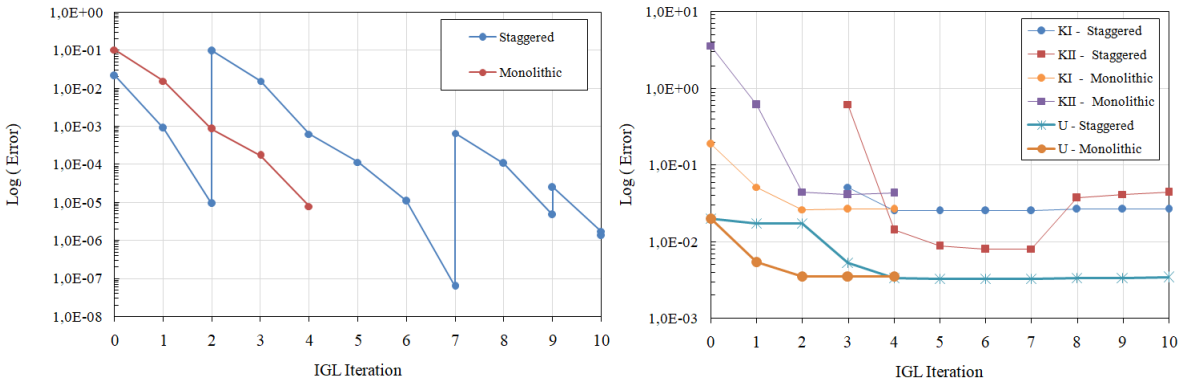

Figure 5. IGL iterations and error evolution. Note that the SIFs are calculated only after the first GFEM^{gl} cycle. This is performed after the iteration 0 for the monolithic strategy and after the iteration 2 for the staggered strategy.

Table 3 shows the reference solutions stress state at the frame corner node and the solutions obtained from the monolithic and staggered procedures. These data were extrapolated from the values calculated at the Gauss integration points of the elements sharing this node. This was necessary because the frame corner point is where the stress field is singular. Therefore, these results are used here for comparison only. An error of 0.31% was observed regarding strain energy for both iterative coupling procedures.

4 Conclusions

This study focuses on the application of the IGL coupling method combined with GFEM and GFEM^{gl} in models with multiple domains, each one represented by a respective mesoscale. The results obtained were satisfactory, with displacement approximation errors in the bar model on the order of 10^{-4} and between 0.12% and 4.38% for the parameters related to the plane model.

Table 3. Stress state of the node located at the corner of the frame - Mesoscale 2

Models	σ_{xx}	Error (%)	σ_{yy}	Error (%)	τ_{xy}	Error (%)
Reference	808.22	-	866.97	-	-355.90	-
Monolithic (1GL)	809.38	0.14	868.01	0.12	-356.36	0.13
Staggered (1GL)	809.36	0.14	867.99	0.12	-356.35	0.13

The IGL strategy was robust to solve problems with multiple local domains, as the iterative convergence process was unaffected. This capability contributes to the broader application of the method in large structures, which often involve numerous local phenomena requiring detailed and appropriately refined models.

Another characteristic of IGL verified in the examples is the capability to analyze structures with different levels of mesh refinement, avoiding to adopt a single model that considers the effects of scales with significantly different magnitudes, which could lead to high computational costs or inadequate representation of localized phenomena.

This is the first part of a work that aims to automate the coupling procedure between the *Abaqus* and *INSANE* solvers. The next step will involve parallelizing the multiple mesoscale solutions instead of the sequential procedure.

Acknowledgements. The authors gratefully acknowledge the importante support of the Brazilian research agencies FAPEMIG (in Portuguese "Fundação de Amparo à Pesquisa de Minas Gerais") - financial support and Grant APQ-01656-18, CNPq (in Portuguese, "Conselho Nacional de Desenvolvimento Científico e Tecnológico") - Grant 308444/2022-1 and CAPES (in Portuguese, "Coordenação de Aperfeiçoamento de Pessoal de Nível Superior").

Authorship statement. The authors hereby confirm that they are the sole liable persons responsible for the authorship of this work, and that all material that has been herein included as part of the present paper is either the property (and authorship) of the authors, or has the permission of the owners to be included here.

References

[1] J. D. Whitcomb. Iterative global local finite element analysis. *Computers & Structures*, vol. 40, n. 4, pp. 1027–1031, 1991.

[2] T. Strouboulis, I. Babuška, and K. Copps. The design and analysis of the Generalized Finite Element Method. *Computer Methods in Applied Mechanics and Engineering*, vol. 181, n. 1-3, pp. 43–69, 2000.

[3] C. A. Duarte and D. J. Kim. Analysis and applications of a generalized finite element method with global-local enrichment functions. *Computer Methods in Applied Mechanics and Engineering*, vol. 197, n. 6–8, pp. 487–504, 2008.

[4] H. Li, P. O'hara, and C. A. Duarte. Non intrusive coupling of a 3 d generalized finite element method and abaqus for the multiscale analysis of localized defects and structural features. *Finite Elements in Analysis and Design*, vol. 193, pp. 103554, 2021.

[5] M. Duval, J. C. Passieux, M. Salaun, and S. Guinard. Non-intrusive coupling: Recent advances and scalable nonlinear domain decomposition. *Archives of Computational Methods in Engineering*, vol. 23, n. 1, pp. 17–38, 2014.

[6] N. A. S. Filho. Implementação não intrusiva do método dos elementos finitos generalizados global-local. Master's thesis, Universidade Federal de Minas Gerais, Belo Horizonte, MG, Brasil, 2023.

[7] A. C. P. Bueno. Implementação não intrusiva do método dos elementos finitos generalizados global-local para simulação de problemas com trincas. Master's thesis, Universidade Federal de Minas Gerais, Belo Horizonte, MG, Brasil, 2024.

[8] H. Li, J. Avecillas-Leon, N. Shauer, and C. A. Duarte. A non intrusive iterative generalized finite element method for multiscale coupling of 3 d solid and shell models. *Computer Methods in Applied Mechanics and Engineering*, vol. 402, pp. 115408, 2022.

[9] B. Szabo and I. Babuška. *Finite Element Analysis*. John Wiley & Sons, Inc., 1991.

[10] N. Moës, J. Dolbow, and T. Belytschko. A finite element method for crack growth without remeshing. *International Journal for Numerical Methods in Engineering*, vol. 46, pp. 131–150, 1999.

[11] G. M. Fonseca. Propagação de trincas em meios elásticos lineares via método dos elementos finitos generalizados com estratégia global local automatizada. Master's thesis, Universidade Federal de Minas Gerais, Belo Horizonte, MG, Brasil, 2019.